In Vitro Mitral Valve Simulator Mimics Systolic Valvular Function of Chronic Ischemic Mitral Regurgitation Ovine Model

Andrew W. Siefert, MS, Jean Pierre M. Rabbah, BS, Kevin J. Koomalsingh, MD, Steven A. Touchton, Jr, BS, Neelakantan Saikrishnan, PhD, Jeremy R. McGarvey, MD, Robert C. Gorman, MD, Joseph H. Gorman, III, MD, and Ajit P. Yoganathan, PhD

The Wallace H. Coulter Department of Biomedical Engineering, Georgia Institute of Technology and Emory University, Atlanta, Georgia; Gorman Cardiovascular Research Group, University of Pennsylvania, Philadelphia, Pennsylvania

Background. **This study was undertaken to evaluate an in vitro mitral valve (MV) simulator's ability to mimic the systolic leaflet coaptation, regurgitation, and leaflet mechanics of a healthy ovine model and an ovine model with chronic ischemic mitral regurgitation (IMR).**

Methods. **Mitral valve size and geometry of both healthy ovine animals and those with chronic IMR were used to recreate systolic MV function in vitro. A2-P2 coaptation length, coaptation depth, tenting area, anterior leaflet strain, and MR were compared between the animal groups and valves simulated in the bench-top model.**

Results. **For the control conditions, no differences were observed between the healthy animals and simulator in coaptation length ($p = 0.681$), coaptation depth ($p = 0.559$), tenting area ($p = 0.199$), and anterior leaflet strain in the radial ($p = 0.230$) and circumferential ($p = 0.364$) directions. For the chronic IMR conditions, no differences were observed between the models in coaptation length ($p = 0.596$), coaptation depth ($p = 0.621$), tenting area ($p = 0.879$), and anterior leaflet strain in the radial ($p = 0.151$) and circumferential ($p = 0.586$) directions. MR was similar between IMR models, with an asymmetrical jet originating from the tethered A3-P3 leaflets.**

Conclusions. **This study is the first to demonstrate the effectiveness of an in vitro simulator to emulate the systolic valvular function and mechanics of a healthy ovine model and one with chronic IMR. The in vitro IMR model provides the capability to recreate intermediary and exacerbated levels of annular and subvalvular distortion for which IMR repairs can be simulated. This system provides a realistic and controllable test platform for the development and evaluation of current and future IMR repairs.**

(Ann Thorac Surg 2013;95:825–30)

In the past decade, the surgical repair of ischemic mitral regurgitation (IMR) has been improved with the implantation of an undersized complete rigid annuloplasty ring and coronary revascularization [1, 2]. Although undersized annuloplasty (UA) is effective in the majority of cases, approximately 10% to 15% of patients have postoperative left ventricular (LV) dilatation with recurrent severe mitral regurgitation (MR) [3, 4]. These patients often present with a severely distended left ventricle whose geometric papillary muscle (PM) distortions impede the ability of UA to sustain coaptation. Although the rates of recurrent MR have been reduced, several issues impede the ability to optimally treat this subset of patients [5].

A primary issue relates to identifying patients who will benefit from isolated UA [5]. Although ventricular and leaflet-based measures have demonstrated significant correlations with patient outcomes, no metrics directly quantify the geometric PM distortions that give allowance or impede the compensatory effects of UA [6–9]. A secondary issue is the need to understand the geometric mechanisms and limits of IMR repairs to improve and assess their suitability for maintaining coaptation with severe or progressive PM displacement. Assessing these issues will aid in identifying patients who may benefit from a given treatment while additionally contributing to the improvement and individualization of treatment modalities [5].

One route toward assessing these clinical issues is through the use of in vitro mitral valve (MV) simulators. These simulators provide the unique advantage of isolating the effect of the relative PM geometry on valvular function, which in humans can be difficult to assess clinically. Moreover, in vitro models provide the versatility to simulate varying degrees of disease, multiple repairs, and simultaneous measures of MV mechanics, which combined can be unfeasible in animal models. Despite these advantages, no bench models have been comprehensively assessed for their ability to emulate in vivo valve function [10–12]. Evaluating this comparison will provide a realistic and controllable test platform for the in vitro development and evaluation of IMR repairs. To this end, the aim of this study was to assess a MV

Accepted for publication Nov 6, 2012.

Address correspondence to Dr Yoganathan, 313 Ferst Dr, Atlanta, GA 30332; E-mail: ajit.yoganathan@bme.gatech.edu.

Published by Elsevier Inc

0003-4975/$36.00
http://dx.doi.org/10.1016/j.athoracsur.2012.11.039

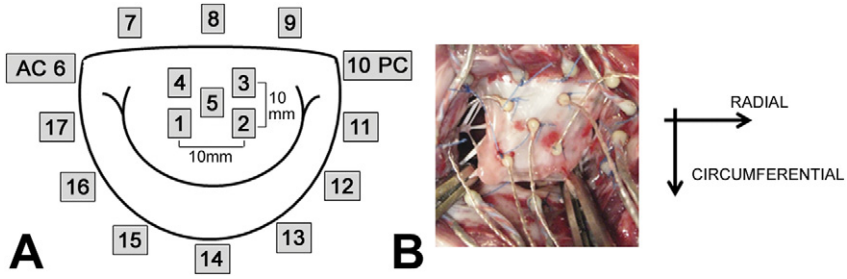

Fig 1. (A) Geometric map of ultrasonomicrometry crystals localized to the A2 anterior leaflet and mitral annulus (AC = anterior commissure; PC = posterior commissure.) (B) In vivo image of crystals localized to the mitral annulus and anterior leaflet with directions of strain shown.

simulator's ability to mimic the systolic leaflet coaptation, MR characteristics, and leaflet mechanics of healthy ovine models and those with chronic IMR.

Material and Methods

Chronic IMR Ovine Model

The animals used in this work received care in compliance with the protocols approved by the Institutional Animal Care and Use Committee at the University of Pennsylvania in accordance with the guidelines for humane care (National Institutes of Health Publication 85-23, revised 1996).

Six Dorsett hybrid sheep received a posterior basal LV infarct to induce progressive chronic IMR. This model has been extensively studied and precisely mimics an inferior LV infarction described in humans [1–3, 13]. Through a sterile left lateral thoracotomy, snares were placed to permanently occlude the proximal second and third obtuse marginal branches of the circumflex coronary artery. After infarction, the thoracotomy was closed and IMR allowed to progress for an 8-week period before evaluating in vivo experimental endpoints.

Ovine Protocol

Control (n = 6) and chronic IMR ovine subjects (n = 6) were intubated, anesthetized, and ventilated with isoflurane and oxygen. Surface electrocardiograms and arterial blood pressure were monitored. A right thoracotomy was performed. On the heart's exposure, epicardial Doppler echocardiographic images were obtained to evaluate MR (Phillips IE33 Matrix; Philips Healthcare, Andover, MA). MR was graded on a 0 to 4+ scale, in which 0 represented no MR and 4+ represented severe MR with reversal of pulmonary vein flow.

Using published techniques, 2-mm hemispheric piezoelectric transducers (Sonometrics Corp, London, Ontario, Canada) were localized to the mitral annulus (n = 12) and A2 anterior mitral leaflet (n = 5) and connected to a Series 5001 Digital Sonomicrometer (Sonometrics Corp) (Fig 1) [13]. For this study, ultrasonomicrometry crystals were not localized to each PM tip. The ability to accurately place transducers on the PM tips can be difficult, and from our experience PM crystals are more prone to failure. For these reasons, we used a historical data set that was successful in capturing the PM positions throughout the cardiac cycle [13]. After weaning each subject from cardiopulmonary bypass, a high-fidelity pressure transducer (± 1 mm Hg) (SPR-3505; Millar Instruments, Houston, TX) was passed percutaneously into the left ventricle through the femoral artery for continuous measurement of left ventricular pressure (LVP). A surface electrocardiogram, LVP, and arterial pressure (Hewlett-Packard78534C monitor; Hewlett-Packard Inc, Santa Clara, CA) were monitored.

On establishing baseline hemodynamics (100 mm Hg peak LVP; 3.3 L/min cardiac output), the 3-dimensional coordinates (resolution of ± 0.024 mm) of each sonometric transducer were recorded at 200 Hz with simultaneous measurements of LVP. After completion of the experiment, animals were euthanized with 1 g thiopental and 80 mEq KCl. Hearts were removed and the left ventricle opened through the interventricular septum to quantify the infarct size as a percentage of the left ventricle [14].

In Vitro Simulator

In vitro simulation was conducted in the extensively studied Georgia Tech left heart simulator (GTLHS) (Fig 2) [12, 15–19]. This closed-loop simulator allows for precise control of annular and subvalvular MV geometry at physiologic left heart hemodynamics. Excised ovine MVs were sutured to an adjustable annulus built to mimic the same size and shape measured in both our healthy and chronic IMR animals (Table 1). The annulus could asymmetrically dilate from a 6.5 cm^2 D-shaped orifice to 10.5 cm^2. The shape of the dilatated annulus was constructed based on the posteromedially dilatated annular geometries in our IMR animals. PM positions were controlled by 2 mechanically adjustable positioning rods capable of achieving positions in the apical, lateral, and posterior directions at a resolution of ± 0.25 mm. Transmitral flow was measured using an electromagnetic probe (FM501D; Carolina Medical Electronics, East Bend, NC) mounted upstream of the atrium. Transmitral pressure was monitored with transducers mounted in the atrium and ventricle (DC-40; Validyne Engineering, Northridge, CA).

Dual-Camera Stereo Photogrammetry

Dual-camera stereo photogrammetry has been used successfully in previous studies to measure MV leaflet and chordal strains in vitro [15, 16]. In this method, tissue dye (Thermo Scientific, Waltham, MA) is used to mark the A2 cusp with a 3 × 3 dot array. During experimentation, 2 synchronized high-speed cameras imaged the marker

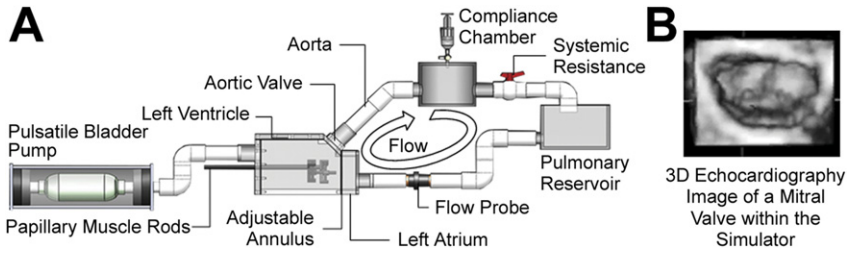

Fig 2. (A) Mitral valve simulator with components identified. (B) Atrial echocardiographic image of mitral valve closure during peak systole within the simulator.

array throughout the cardiac cycle at 500 Hz. From the recorded images, direct linear transformation was used to calculate the 3-dimensional (3D) coordinates of each marker [15, 16]. These coordinates were subsequently used to calculate the strain for the dye-marked region of the anterior leaflet.

In Vitro Protocol

Fresh ovine hearts were obtained and MVs excised (n = 6) preserving their annular and subvalvular anatomy. MVs with an anterior leaflet height of 18 to 19 mm (as measured in our ovine animals) (Table 1), with type I or II PMs, and with all leaflet chordae inserting directly into each PM were selected for experimentation. Selected MVs were sutured to the simulator's annulus using a Ford interlocking stitch. For control conditions, the annulus was set to an area of 6.5 cm^2 and the annular height to a commissural width ratio of 15% as measured in vivo (Table 1). During valve suturing, care was taken to place each suture just above the valve's natural hinge and not through the leaflet tissue. Additionally, normal annular leaflet geometric relationships were respected—the anterior leaflet occupying one third of the annular circumference and the commissures aligned in the 2 and 10 o'clock positions.

After annular suturing, each PM was attached to the PM control rods. Each PM was carefully positioned and fine-tuned to establish the control MV geometry as previously described [19]. Transmitral ovine pulsatile conditions were simulated (cardiac output, 3.3 L/min, 120 beats/min, 100 mm Hg transmitral pressure). Mitral coaptation was then inspected by echocardiography such that the anterior leaflet spanned approximately two thirds of the A2-P2 diameter and the coaptation length was approximately 4 to 5 mm as measured in our healthy animals (Table 2). If the control valve geometry conditions were successfully achieved, transmitral hemodynamics, 3D echocardiography (Philips IE-33), and dual-camera high-speed images of the valve were acquired.

To simulate a chronic IMR MV geometry, the valve annulus was flattened and asymmetrically dilated per the mean valvular distortions measured in our chronic IMR animals (Table 1). The PMs were adjusted per the displacements observed between identical healthy and chronic IMR models [13]. Based on these data, the posteromedial PM was displaced 4 mm laterally, 6 mm posteriorly, and 2 mm basally, whereas the anterolateral PM was displaced 2 mm laterally, 1 mm anteriorly, and 1.5 mm apically. After the displacement of each PM, transvalvular hemodynamics were established and experimental endpoints recorded.

Data and Statistical Analysis

Ultrasonomicrometry and tissue dye coordinates acquired in both the animal and bench experiments were used to compute the anterior leaflet strain. Using a custom MATLAB program (Mathworks, Natick, MA), biquintic finite element interpolation was used to fit a surface to the recorded 3D marker coordinates [15, 16, 20]. Generated surfaces were used to determine the radial and circumferential strains and strain rates endured by the anterior leaflet [15]. Similar to previous studies, the referential leaflet strain configuration corresponded with the minimum LVP. All in vitro hemodynamic data were processed offline within a custom MATLAB program and averaged more than 10 consecutive cardiac cycles. In vitro regurgitation fractions were calculated as the total retrograde volume divided by the stroke volume. Echocardiographic data were analyzed using Philips QLAB, version 7.0 (Philips Healthcare, Andover, MA). To compare between animal groups and simulated conditions, a nonparametric Mann-Whitney *U* test was used. In vitro comparisons made between the control and chronic IMR conditions were completed with Wilcoxon's signed-rank test. All statistical analyses were completed using SPSS, version 20 (IBM Corp, Armonk, NY). Endpoints are expressed as a mean ± 1 standard deviation.

Results

Animal Characteristics

Baseline characteristics of the control and chronic IMR animals are presented in Table 1. Both animal groups

Table 1. Baseline Characteristics of the Ovine Subjects

Group	Weight (kg)	Heart Rate (beats/min)	Peak LVP (mm Hg)	dLVP/dt (mm Hg)	Infarcted LV Endocardium (%)	Anterior Leaflet Height (cm)	Mitral Annular Area (cm^2)
Control	38 ± 2	98 ± 15	103 ± 6	1842 ± 493	0	1.8 ± 0.1	6.4 ± 1.2
Chronic IMR	39 ± 2	100 ± 13	101 ± 8	1592 ± 490	18.5 ± 1.6	1.9 ± 0.1	10.4 ± 2.2

dLVP/dt = derivatives of left ventricular pressure; IMR = ischemic mitral regurgitation; LV = left ventricular; LVP = left ventricular pressure.

Table 2. A2-P2 Coaptation Characteristics Between the Animal and Simulated Valves

Condition	Coaptation Length (mm)	Coaptation Depth (mm)	Tenting Area (cm^2)
Control animal simulator	4.4 ± 0.4	1.8 ± 0.2	0.23 ± 0.07
Control Sim	4.0 ± 0.4	2.1 ± 0.3	0.16 ± 0.05
cIMR Animal	3.2 ± 0.3	2.4 ± 0.8	0.27 ± 0.13
cIMR Sim	3.1 ± 0.6[a]	2.8 ± 1.0[a]	0.31 ± 0.13[a]

[a] Denotes a $p < 0.05$ significant difference between the chronic IMR and control simulated conditions.

cIMR = chronic ischemic mitral regurgitation; IMR = ischemic mitral regurgitation; Sim = simulated valve.

exhibited similar weights, heart rate, peak LVP, and anterior leaflet heights. Similar to previous studies, the chronic IMR animals exhibited a reduced rate of change of LVP during isovolumetric contraction dLVP/dt and mitral annular area increase of approximately 60% as modeled within the in vitro simulator [13].

The simulation of the chronic IMR valve geometry was a direct function of the annular perturbations measured in our animals and the relative PM displacements determined from previous data [13]. From these data, the posteromedial PM was observed to have a mean relative displacement of 7.25 mm laterally, 10.05 mm posteriorly, and 1.75 mm basally, whereas the anterolateral PM exhibited a mean relative displacement of 4.04 mm laterally, 1.28 mm anteriorly, and 3 mm apically. These relative displacements were similar to those observed previously by Tibayan and colleagues [21]. In pilot studies, the use of these absolute displacements resulted in PM chordal tearing. We believe this tearing was a consequence of using postmortem tissue, whereas in vivo the MV is distended over a longer time (8 weeks) and has exhibited the capacity to actively remodel [22, 23]. For these reasons, intermediary levels of these displacements were used (see Methods section).

Comparison of Coaptation

Leaflet coaptation across the A2-P2 annular diameter was evaluated for coaptation length, coaptation depth, and tenting area. Measured values within each animal group were compared with those measured within the simulated conditions. For the control conditions, no significant differences were observed between the healthy animals and the MV simulator in coaptation length ($p = 0.681$), coaptation depth ($p = 0.559$), and tenting area ($p = 0.199$) (Table 2). Similarly for the chronic IMR conditions, no differences were observed between models in coaptation length ($p = 0.596$), coaptation depth ($p = 0.621$), and tenting area ($p = 0.879$). Although not reaching statistical significance, coaptation length was consistently lower in the simulated conditions as verified by the comparatively greater coaptation depth.

To demonstrate changes in coaptation within the GTLHS, each measure of coaptation was compared between the simulated control and the chronic IMR conditions. Results revealed the coaptation length to significantly decrease from the control to chronic IMR condition ($p = 0.027$) across the A2-P2 annular diameter. Additionally, coaptation depth ($p = 0.046$) and tenting area ($p = 0.028$) were observed to significantly increase with simulated chronic IMR (Table 2).

Comparison of MR

MR was assessed between the chronic IMR animals and simulated conditions. Within the animal group, observed MR was consistent with previous studies, reaching a mean grade of 3.17 ± 0.75 [13]. For the simulated conditions, MR was quantified by direct measurement using an electromagnetic flow probe. The mean in vitro MR fraction was found to reach 46% ± 6% and a mean grade of 3+. In comparison with the chronic IMR animals, in vitro MR jets were observed to be asymmetrical and to originate from the tethered A3-P3 leaflets.

Comparison of Anterior Leaflet Mechanics

For control conditions, no significant differences were observed in the A2 leaflet strain between the control animals and simulated conditions in the radial (21% ± 14% versus 32% ± 18%; $p = 0.230$) and circumferential (6% ± 10% versus 11% ± 7%; $p = 0.364$) directions. Similarly, no significant differences were observed between the chronic IMR animals and simulated IMR conditions in the radial (21% ± 11% versus 34% ± 18%; $p = 0.151$) and circumferential (7% ± 9% versus 9% ± 7%; $p = 0.586$) directions, respectively. To determine if leaflet strain increases from a control to chronic IMR valve geometry, radial and circumferential strains were compared between the simulated conditions. In comparison with the control condition, results revealed a significant increase in radial ($p = 0.028$) and circumferential ($p = 0.028$) strains.

In addition to the peak measured values, the peak rate change of these strains [d(ε)/dt] were determined during isovolumetric contraction and compared between animal and simulation groups. Because these values are largely a function of the rate at which LVP increases, all d(ε)/dt values were normalized by d(LVP)/dt (Table 3). Results revealed no significant differences between the control animals and simulated control conditions in the radial

Table 3. Normalized Strain Rate

	Normalized Strain Rate (mm/(mm × mm Hg) × 100%	
Group	Radial	Circumferential
Control animal simulator	0.24 ± 0.21	0.20 ± 0.13
Control Sim	0.23 ± 0.05	0.11 ± 0.07
cIMR Animal	0.30 ± 0.18	0.20 ± 0.13
cIMR Sim	0.52 ± 0.14[a]	0.16 ± 0.06[b]

[a] Denotes a $p < 0.01$ significant difference between the chronic IMR and control simulated conditions; [b] denotes a $p < 0.05$.

cIMR = chronic ischemic mitral regurgitation; IMR = ischemic mitral regurgitation; Sim = simulated valve.

($p = 0.873$) and circumferential ($p = 0.109$) directions, respectively. Similar results were observed between the chronic IMR animals in the radial ($p = 0.631$) and circumferential ($p = 0.200$) directions. To determine if leaflet strain rate increases from a control to chronic IMR valve geometry, radial and circumferential strain rates were compared between the simulated conditions. In comparison to the control condition, results revealed a significant increase in the normalized radial ($p = 0.005$) and circumferential ($p = 0.018$) strain rates.

Comment

Simulated changes in systolic MV geometry from control to chronic IMR were modeled within the GTLHS. With a chronic IMR MV geometry, significant decreases in coaptation length and significant increases in coaptation depth and tenting area were observed as clinically described [1–4]. These changes in leaflet coaptation were accompanied with MR jets of a magnitude similar to that observed in the ovine subjects. In comparison to the simulated controls, a chronic IMR MV geometry resulted in significantly increasing both radial and circumferential anterior leaflet strains. This can be explained in that the IMR geometry increases the leaflet area exposed to the transmitral pressure, resulting in a greater force and stretch within the tissue.

The annular MV geometric changes and MR observed within our animals are in excellent agreement with previous studies [13, 14, 24, 25]. Because the coronary anatomy varies very little between sheep and they do not form collateral vessels, these sheep provide a reliable and repeatable model of chronic IMR [24]. Because of the precise control that is allowed by the simulator's components, the simulated annular dilatation and PM displacement is also very repeatable. During valve selection, great care was given to selecting valves of a size similar to those in vivo. Although similar in size, the number of chordae per valve likely differed, as did their geometric insertions to the PMs and leaflets. Even with this variability, the standard deviations found in the in vitro MR fractions, coaptation characteristics, and strain was improved in comparison with previous studies [12, 15, 26, 27].

Given the consistency of both models, the authors believe that demonstrating negative results with a larger sample size would still not supersede or overcome the limitations of the in vitro simulator. For these reasons, we believe the negative results reported herein are meaningful and highlight the unique ability of the simulator to mimic the systolic valvular distortions, coaptation, and anterior leaflet strain of a chronic IMR ovine model. These results additionally demonstrate the repeatability of the simulator and its ability to detect small differences between experimental conditions that can be difficult in animal or human studies.

For type IIIb dysfunction, the ultimate goals are to stop MR and promote reverse LV remodeling [1, 2]. The effectiveness of IMR repairs is dependent on the repair's ability to compensate for the distended left ventricle by restoring coaptation and stopping MR during systolic closure [3–5]. For these reasons, the ultimate goal of our simulator is to mimic the systolic closure of the leaflets and moreover to understand how to improve it. Hence, the ultimate goal of our simulator is to mimic the systolic closure of the leaflets and provide a platform to investigate how to improve it in repair conditions.

Provided the advantages of the described simulator, several limitations are associated with both the apparatus and the methodologies used in this study. The described MV simulator can recreate the systolic geometric configuration of the MV but at present does not incorporate the intricate mechanics associated with valve-ventricle interaction. Its inclusion would likely increase the accuracy of mimicking the dynamic in vivo valve function, the effects of which should be isolated in future studies. Although at present the model can focus on the geometry of the annulus, leaflets, and PMs, evaluating repairs that directly affect the ventricle will require appropriate in vivo geometric boundary conditions.

In this study, the comparison of our simulated results is limited to an extensively studied inferior IMR ovine model and does not emulate the valvular distortion and function that may be seen in other causes. The IMR ovine model's resulting valvular geometry is likely dependent on infarct size and may change with a lesser or greater degree of myocardial infarction. The evaluation of leaflet coaptation was limited to the A2-P2 annular plane because the ability to quantify coaptation along the A3-P3 plane was limited because of the thin, ill-coapting leaflets. In future studies, a broader spectrum of IMR valvular geometries (ie, from more diffuse coronary disease or anterolateral infarction) should be simulated, with similarities assessed between the in vitro and in vivo models. Dynamic leaflet motion within the simulator should additionally be evaluated.

In our studied animals, implantation of the miniature ultrasonomicrometry transducers to the anterior leaflet likely influenced the local deformation of the anterior leaflet and could be improved with the use of radiopaque markers. For the computation of A2 leaflet strain, the number of transducers that could be localized to the ovine anterior leaflet was limited to 5, whereas the GTLHS strain was computed with 9. Although statistically significant differences between the measured aspects were not observed, we believe the differences in the magnitudes between each metric are representative of those that may be observed with a larger sample size. Combined, these limitations must be assessed in coordination with the results of future studies that use the tested IMR valve geometry as a platform to evaluate MV repairs.

Our findings in this study demonstrate the ability of an in vitro simulator to mimic A2-P2 leaflet coaptation, anterior leaflet strain, and MR characteristics of healthy and chronic IMR ovine animals at peak systole. These results provide a foundation to evaluate the effect of IMR MV geometry on the effectiveness of current and future IMR repairs. A study is currently under way to examine the compensatory limits of undersized mitral annulo-

plasty and the effectiveness of ventricular-based techniques in restoring coaptation. With additional investigation, these findings should provide key insight into the effect of MV geometry on repair effectiveness and contribute to our clinical understanding of the geometry-based mechanisms that restore valvular competence.

This study was supported by a research grant awarded from the National Institute of Health (R01 HL090661-02) and from the National Heart and Lung Institute (HL063954, HL073021, HL103723, and HL108330). Robert Gorman and Joseph Gorman were supported by individual Established Investigator Awards from the American Heart Association.

References

1. Braun J, van de Veire NR, Klautz RJM, et al. Restrictive mitral annuloplasty cures ischemic mitral regurgitation and heart failure. Ann Thorac Surg 2008;85:430–7.
2. Geidel S, Lass M, Schneider C, et al. Downsizing of the mitral valve and coronary revascularization in severe ischemic mitral regurgitation results in reverse left ventricular and left atrial remodeling. Eur J Cardiothorac Surg 2005;27:1011–6.
3. Kuwahara E, Otsuji Y, Iguro Y, et al. Mechanism of recurrent/persistent ischemic/functional mitral regurgitation in the chronic phase after surgical annuloplasty. Circulation 2006;114:I-229–I-534.
4. McGee EC, Gillinov AM, Blackstone EH, et al. Recurrent mitral regurgitation after annuloplasty for functional ischemic mitral regurgitation. J Thorac Cardiovac Surg 2004;128:916–24.
5. Braun J, Klautz RJM. Mitral valve surgery in low ejection fraction, severe ischemic mitral regurgitation patients: should we repair them all? Curr Opin Cardiol 2012;27:111-–7.
6. Ciarka A, Braun J, Delgado V, et al. Predictors of mitral regurgitation recurrence in patients with heart failure undergoing mitral valve annuloplasty. Am J Cardiol 2010;106:395–401.
7. Mange J, Pibarot P, Dagenais F, Hachicha Z, Dumesnil JG, Sénéchal M. Preoperative posterior leaflet angle accurately predicts outcome after restrictive mitral annuloplasty for ischemic mitral regurgitation. Circulation 2007;115:782–91.
8. Lee APW, Acker M, Kubo S, et al. Mechanisms of recurrent functional mitral regurgitation after mitral valve repair in nonischemic dilated cardiomyopathy: importance of distal anterior leaflet tethering. Circulation 2009;119:2606–14.
9. Buckley O, Di Carli M. Predicting benefit from revascularization in patients with ischemic heart failure: imaging of myocardial ischemia and viability. Circulation 2011;123:444–50.
10. Vismara R, Pavesi A, Votta E, Taramasso M, Maisano F, Fiore GB. A pulsatile simulator for the in vitro analysis of the mitral valve with tri-axial papillary muscle displacement. Int J Artif Organs 2011;34:383–91.
11. Bhattacharya S, He Z. Annulus tension of the prolapsed mitral valve correction by edge-to-edge repair. J Biomech 2012;45:562–8.
12. He S, Jimenez JH, He Z, Yoganathan AP. Mitral leaflet geometry perturbations with papillary muscle displacement and annular dilation: an in-vitro study of ischemic mitral regurgitation. J Heart Valv Dis 2003;12:300–7.
13. Gorman JH III, Gorman RC, Jackson BM, Enomoto Y, St. John-Sutton MG, Edmunds LH, Jr. Annuloplasty ring selection for chronic ischemic mitral regurgitation: lessons from the ovine model. Ann Thorac Surg 2003;76:1556–63.
14. Robb JD, Minakawa M, Koomalsingh, KJ, et al. Posterior leaflet augmentation improves leaflet tethering in repair of ischemic mitral regurgitation. Eur J Cardiothorac Surg 2011;40:1501–7.
15. He Z, Ritchie J, Grashow JS, Sacks MS, Yoganathan AP. In vitro dynamic strain behavior of the mitral valve posterior leaflet. J Biomech Eng 2005;127:504–11.
16. Padala M, Sacks MS, Liou SW, Balachandran K, He Z, Yogantahn AP. Mechanics of the mitral valve strut chordae insertion region. J Biomech Eng 2010;132:081004.
17. Rabbah JP, Siefert AW, Spinner EM, Saikrishnan N, Yoganathan AP. Peak mechanical loads induced in the in-vitro edge-to-edge repair of posterior leaflet flail. Ann Thorac Surg 2012;94:1445–52.
18. Nielsen SL, Nygaard H, Fontaine AA, et al. Chordal force distribution determines systolic mitral leaflet configuration and severity of functional mitral regurgitation. J Am Coll Cardiol 1999;33:843–53.
19. Jimenez JH, Soerensen DD, He Z, et al. Effects of a saddle shaped annulus on mitral valve function and chordal force distribution: an in vitro study. Ann Biomed Eng 2003;31:1171–81.
20. Sacks MS, Enomoto Y, Graybill JR, et al. In vivo dynamic deformation of the mitral valve anterior leaflet. Ann Thorac Surg 2006;82:1369–78.
21. Tibayan FA, Rodriguez F, Zasio MK, et al. Geometric distortions of the mitral valvular-ventricular complex in chronic ischemic mitral regurgitation. Circulation 2003;108:II-116–21.
22. Rausch MK, Tibayan FA, Miller DC, Kuhl E. Evidence of adaptive mitral leaflet growth. J Mech Behavior Biomed Mater 2012;15C:208–17.
23. Dal-Bianco JP, Aikawa E, Bischoff J, et al. Active adaptation of the tethered mitral valve: insights into a compensatory mechanism for functional mitral regurgitation. Circulation 2009;120:334–42.
24. Llaneras MR, Nance ML, Streicher JT, et al. Large animal model of ischemic mitral regurgitation. Ann Thorac Surg 1994;57:432–9.
25. Gorman JH, Jackson BM, Enomoto Y, Gorman RC. The effect of regional ischemia on mitral valve annular saddle shape. Ann Thorac Surg 2004;77:544–8.
26. Nielsen SL, Nygaard H, Mandrup L, et al. Mechanism of incomplete mitral leaflet coaptation-interaction of chordal restraint and changes in mitral leaflet coaptation geometry. Insight from in vitro validation of the premise of force equilibrium. J Biomech Eng 2002;124:596–608.
27. He S, Lemmon JD, Weston MW, Jensen MO, Levine RA, Yoganathan AP. Mitral valve compensation for annular dilatation: in vitro study into the mechanisms of functional mitral regurgitation with an adjustable annulus model. J Heart Valve Dis 1999;8:294–302.